Trends Phytochem. Res. 4(3) 2020 109-116

Trends in Phytochemical Research (TPR)

Journal Homepage: http://tpr.iau-shahrood.ac.ir

Original Research Article

A new pyrrolidinyl-piperazine alkaloid derivative from *Oxyanthus speciosus* DC. (Rubiaceae)

JUDITH CAROLINE NGO NYOBE[1]✉*, DÉSIRÉ MAMA BIKÉLÉ[1], MATIEDJIE BECKY FODOUOP[2], EMMANUEL MPONDO MPONDO[2] AND JEAN-CLAUDE NDOM[1]✉*

[1]Analytical, Structural and Materials Chemistry Laboratory, Department of Chemistry, Faculty of Science, University of Douala, P.O. Box 24157, Douala, Cameroon

[2]Department of Pharmaceutical Sciences, Faculty of Medicine and Pharmaceutical Sciences, University of Douala, P.O. Box 24157, Douala, Cameroon

ABSTRACT

A new pyrrolidinyl-piperazine alkaloid derivative named 2-(7′-methylhexyloxy)furan-5′-yl)-6-(pyrrolidin-7-yl)piperazine (**1**), along with five known compounds were isolated from methanolic extract of the roots of *Oxyanthus speciosus* DC. (Rubiaceae). The structure of this new alkaloid was elucidated on the basis of the relevant NMR and MS analyses. Compound (**1**) possesses potent *in vitro* anti-inflammatory activity by protein denaturation assay with an IC_{50} value of 1.930 ± 0.9123 µg/mL. The obtained results indicated that the crude methanolic extract of *O. speciosus* DC. roots and its isolated pyrrolidinyl-piperazine alkaloid have potentials for further development as an effective and natural anti-inflammatory agents.

ARTICLE HISTORY

Received: 18 December 2019
Revised: 24 March 2020
Accepted: 08 July 2020
ePublished: 05 September 2020

KEYWORDS

Anti-inflammatory activity
Oxyanthus speciosus DC
Rubiaceae
2-(7'-methylhexyloxy)-furan-5'-yl-6-(pyrrolidin-7-yl)piperazine

1. Introduction

As a part of our continuing phytochemical research for exploring bioactive molecules from Cameroonian plants, *Oxyanthus speciosus* DC. (Rubiaceae) was studied. The investigation of this plant was motivated since the decoction prepared from its leaves is widely used to treat snake bites, lower fever, stomach and pulmonary ailments, while the roots and stem bark are used to treat snake bites. In addition, twigs and flower buds of this herbal species are applied traditionally against fever, toothache and jaundice (Raponda-Walker et al., 1961; Aké Assi et al., 1985; Adjonohoun et al., 1988; Kokwaro et al., 1993; Burkill et al., 1997; Neuwinger et al., 2000). This plant also exhibits promising antimycobacterial activities (Aro et al., 2015, 2019a) and can be utilized to relieve abdominal pain (Bouquet, 1969). Until now, no phytochemical study has been reported on the roots of *O. speciosus* DC. (Fig. 1). According to the previous phytochemical studies, the leaves and stem barks of *O. pallidus* evidenced respectively the presence of cycloartane glycosides (Nzedong et al., 2010) and iridoids (Nzedong et al., 2012). Besides, the leaves and stems of *O. pyriformis* subsp. *pyriformis* and *O. speciosus* subsp. *gerrardii* had delivered cyanogenic glycosides (Rockenbach et al., 1992), while *O. speciosus* subsp. *stenocarpus* has highlighted phenolic compounds and triterpenes (Nahrstedt et al., 1995; Aro et al., 2019b). *O. speciosus* DC. distributed in tropical Africa, is an evergreen shrub or a tree up to 14 m tall, with horizontal glabrous branches and bark smooth. It possesses large and beautifully veined, brilliantly glossy leaves and compact clusters of showy, delicate pure-white flowers with long, slim tubes and small petals. Likely, the thick-skinned and spindle-shaped fruits are favorites foods

✉Corresponding authors: Judith Caroline Ngo Nyobe and Jean-Claude Ndom
Tel: (237)690047473; (237)699109480 ; Fax: (237)690047473; (237)699109480
E-mail address: njudithcaroline@yahoo.fr; ndomjefr@yahoo.fr

for fruit eating birds in nature. The specific epithet *spe ciosus* means showy or good looking and refers to the-aesthetically pleasing qualities of the trees (Adjonohoun et al., 1988). This paper reports the structural elucida tion of a new pyrrolidinyl-piperazine alkaloid derivative named (2-(7′-methylhexyloxy)-furan-5′-yl-6-(pyrrolidin-7-yl)piperazine) from the roots of *O. speciosus* DC. (**1**) (Fig. 2) for the first time together with five known compounds, namely aridanin (**2**), hexadecanoic acid (**3**), taraxeryl acetate (**4**), betulinic acid (**5**), taraxerol (**6**), as well (Fig. 3). The anti-inflammatory activities of compound (**1**) and the methanol extract are also presented.

2. Experimental

2.1. General instrumentation

Optical rotation $[\alpha]_D$ (in MeOH, C in g mL^{-1}) was determined at 20 °C by using a JASCO digital polarimeter (model P-1030). The uncorrected melting points were determined on a Buchi apparatus. All the relevant IR and ESIMS spectra were recorded on a Perkin-Elmer 727B spectrometer using KBr pellets as well as Finnigan LCQ having a Rheos 4000 quaternary pump (Flux Instrument), respectively.

The ^1H and ^{13}C NMR spectra were recorded on a Bruker Avance III 500 MHz NMR spectrometer (Rheinstetten, Germany) equipped with a 5 mm cryogenic DCH ($^1H/^{13}C$) probe. Chemical shifts are reported in parts per million (δ) using TMS as the internal standard (δ 0.00 ppm), respectively and the respective coupling constants (*J*) are reported in Hz. For NMR analysis, compound (**1**) was dissolved in $CDCl_3$, while compounds **2-6** were dissolved in CD_2Cl_2.

The HREIMS were obtained on a Q Exactive Plus Hybrid quadrupole-orbitrap mass spectrometer (Thermo Scientific, Waltham, MA, USA) using electro-spray ionization in the positive-ion mode. The spray voltage was set at 3.5 kV; the sheath gas flow rate (N_2) at 50 units; the capillary temperature at 320 °C; the S lens RF level at 50; and the probe heater temperature at 425 °C. EIMS (Electron Impact Mass Spectrometry) were recorded on a Finnigan MAT 95 spectrometer (70 eV) with perfluorokerosene as reference substance.

Column chromatography was carried out on silica gel 60 (70-230 mesh, Merck) and flash silica gel (230-400 mesh, Merck). TLC was performed on Merck precoated silica gel 60 F254 aluminium foil, using ceric sulphate spray reagent and UV lamp at 254 and 365nm for visualization. All reagents used were of analytical reagents grade and used without further purification.

2.2. Plant material

Oxyanthus speciosus DC. was located at 5°27′0″ North longitude, 10°4′0″ East latitude. Their roots were collected in July 2017 at Bangwa in the West Region of Cameroon and identified by Victor Nana, botanist. The voucher specimen N° 56388HN/CAM were deposited at the National Herbarium (Yaounde, Cameroon).

2.3. Extraction and isolation

1.6 kg of the roots of *O. speciosus* were coarsely powdered and macerated with methanol for 72 hours at room temperature. The extract was concentrated under reduced pressure to prepare 113.1 g of a dark brown crude extract. A 100.0-g portion of the dry crude extract was dissolved in 50 mL of methanol and adsorbed on 56.0 g of silica gel 60 (70-230 mesh) for the preparation of slurry. The slurry was air-dried and chromatographed over 350 g of silica gel column (1.6 m x 16 mm x 2 mm) packed using 800 mL of *n*-hexane. The column was eluted successively in increasing order of polarity in various combinations with *n*-hexane, *n*-hexane-CH_2Cl_2 (95:5 to 0:100, v/v) and CH_2Cl_2-MeOH (95:5 to 0:100, v/v). The fractions were collected separately and matched by TLC to check homogeneity. Similar fractions having the same Rf values were combined leading to ten sub-fractions (F1-F10). The pure compounds were obtained after further purification on column chromatography following by direct recrystallization.

2.3.1. Isolation of phytoconstituents of the roots of *O. speciosus*

2.3.1.1. 2-(7′-methylhexyloxy)furan-5′-yl)-6-(pyrrolidin-7-yl)piperazine) (**1**)

Sub-fraction F7 (1.5 g) eluted with hexane-CH_2Cl_2 (20:80, v/v) was column chromatographed on silica gel using 2 L of hexane-CH_2Cl_2 (15:85, v/v) to afford a white amorphous powder of (**1**), yield 20.5 mg, UV λmax (MeOH): 254 nm; m.p. 81.2 °C; [α]D-11.2°; IR νmax (KBr): 3341, 1550 cm^{-1}; ^1H NMR ($CDCl_3$): 7.58 (1H, d, *J* = 5.8 Hz, H-3′), 7.73 (1H, dd, *J* = 5.8, 3.3 Hz, H-4′), 4.64 (1H, dt, (*J* = 7.5, 6.3 Hz, H-7); δ 4.51 (1H, dt, *J* = 6.2, 3.1 Hz, H-2), 4.35 (1H, dt, *J* = 6.5, 3.3 Hz, H-6), 4.22 (2H, dd, *J* = 5.7, 11.4 Hz , H-6′), 2.47 (1H, m, H-5a), 2.37 (2H, m, H-9), 2.22 (1H, m, H-3a), 2.14 (1H, m, H-5b), 2.05 (1H, m, H-3b), 1.28 (2H, m, H-11), 1.27 (2H, m, H-10′), 1.24 (2H, m, H-9′), 1.70 (1H, m, H-7′), 1.33 (2H, m, H-8′), 1.18 (2H, m, H-10), 0.95 (3H, t, *J* = 7.1 Hz, Me-11′), 0.93 (3H, d, *J* = 7.9 Hz, Me-12′); ^{13}CNMR ($CDCl_3$): δ 168.1 (C-2′), 133.2 (C-5′), 130.9 (C-4′), 128.8 (C-3′), 68.5 (C- 6′), 57.8 (C-7), 56.8 (C-2), 55.8 (C-6), 47.1 (C-5), 46.3 (C-3), 45.5 (C-9), 39.3 (C-7′), 30.9 (C-10), 30.2 (C-11), 29.4 (C-10′), 24.3 (C-8′), 23.5 (C-9′), 14.3 (Me-12′), 11.3 (Me-11′), HRESIMS *m/z* 336.2575 [M+H]+, *m/z* 358.2395 $[M+Na]^+$, $C_{19}H_{33}N_3O_2$ (Fig. S1)**.** EIMS *m/z* (rel. int.): 279 (100%), 150 (75%) (Fig. S2)**.**

2.3.1.2. Aridanin (**2**)

Sub-fraction F8 (4.7 g) eluted with CH_2Cl_2-MeOH (30:70, v/v) was column chromatographed on Si gel using CH_2Cl_2-MeOH (40:60, v/v) to give white crystal of (**2**) yield 7.5 mg, m.p. 274-276 °C; ^{13}C-NMR (CD_2Cl_2; 125 MHz): δ 180.1 (C-28), 144.7 (C-13), 122.3 (C-12), 89.1 (C-3), 55.7 (C-5), 47.9 (C-9), 46.6 (C-17), 46.4 (C-19), 42.1 (C-14), 41.9 (C-18), 39.6 (C-8), 39.1 (C-4), 38.5 (C-1), 36.9 (C-10), 34.1 (C-21), 33.3 (C-7), 33.2 (C-29), 33.1 (C-22), 30.9 (C-

Fig. 1. The photograph of the roots of *Oxyanthus speciosus* DC.

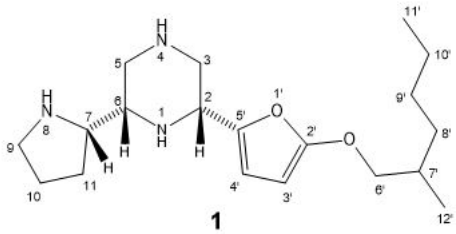

Fig. 2. Molecular structure of (2-(7'-methylhexyloxy)furan-5'-yl)-6-(pyrrolidin-7-yl) piperazine) (**1**).

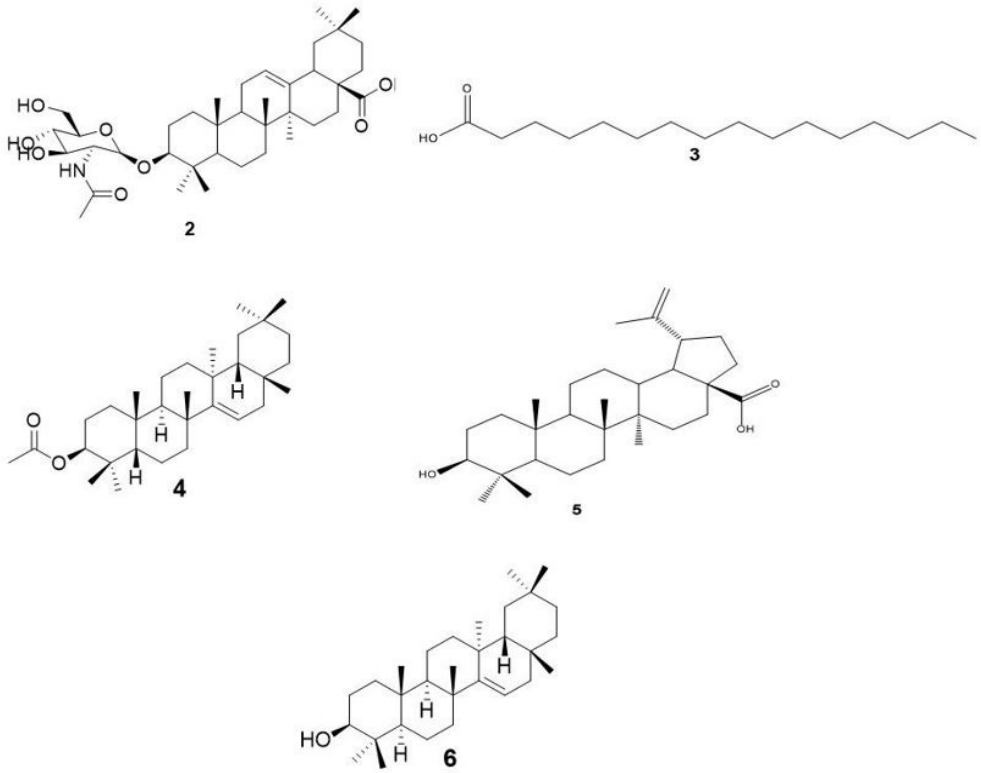

Fig. 3. Molecular structures known of com.p.ounds from *O. speciosus* DC.

20), 28.2 (C-23), 28.1 (C-27), 26.2 (C-2), 26.1 (C-15), 23.8 (C-16), 23.7 (C-30), 23.6 (C-11), 18.4 (C-6), 17.3 (C-26), 16.9 (C-24), 15.4 (C-25), sugar: δ 168.6 (NHCO), 104.7 (C-1′), 77.2 (C-5′), 74.4 (C-3′), 71.2 (C-4′), 61.2 (C-6′), 56.3 (C-2′), 23.5 (CH_3-CO) (Olajide et al., 2019).

2.3.1.3. Hexadecanoic acid (**3**)

Sub-fraction F1 (5.5 g) eluted with hexane-CH_2Cl_2 (90:10, v/v) was column chromatographed on Si gel using hexane-CH_2Cl_2 (97.5:2.5, v/v) to produce a white powder of (**3**), yield 12.4 mg (**3**), m.p. 78.0-80 °C; ^{13}C-NMR (CD_2Cl_2; 125 MHz): δ 179.2 (C-1), 34.0 (C-2), 30.2 (C-3), 29.1-29.9 (C-4 to C-13), 28.9 (C-14), 22.7 (C-15), 14.1 (C-16) (Neoh et al., 2010).

2.3.1.4. Taraxeryl acetate (**4**)

Further elution using hexane-CH_2Cl_2 (95:5, v/v) afforded a white powder of (**4**), yield 10.6 mg; m.p. 302-304 °C; ^{13}C-NMR (CD_2Cl_2; 125MHz): δ 154.8 (C-20), 107.1 (C-30), 80.9 (C-3), 55.4 (C-5), 51.0 (C-9), 48.8 (C-18), 41.9 (C-14), 41.2 (C-8), 39.6 (C-19), 38.8 (C-16), 38.7 (C-13), 38.2 (C-22), 38.1 (C-1), 37.7 (C-4), 37.0 (C-10), 34.7 (C-17), 33.9 (C-7), 27.9 (C-23), 26.6 (C-15), 26.1 (C-12), 25.6 (C-29), 25.5 (C-21), 23.6 (C-2), 21.4 (C-11), 19.8 (C-28), 18.1 (C-6), 16.4 (C-24), 16.3 (C-26), 15.8 (C-25), 14.7 (C-27) (Trinh et al., 2008).

2.3.1.5. Betulinic acid (*5*)

Sub-fraction F_3 (10.7 g) eluted with hexane-CH_2Cl_2 (70:30, v/v) was column chromatographed on Si gel using hexane-CH_2Cl_2 (7.5:2.5, v/v) to afford a colorless amorphous powder of (**5**), yield 7.6 mg; m.p. 317 to 319 °C; ^{13}C-NMR (CD_2Cl_2; 125 MHz): δ 178.9 (C-28), 152.5 (C-20), 110.0 (C-29), 78.2 (C-3), 56.7 (C-17), 56.0 (C-5), 51.0 (C-9), 49.8 (C-19), 47.8 (C-18), 42.9 (C-14), 41.2 (C-8), 39.6 (C-4), 39.3 (C-1), 38.7 (C-13), 37.6 (C-22), 37.5 (C-10), 34.9 (C-7), 32.9 (C-16), 31.3 (C-15), 30.3 (C-21), 28.7 (C-23), 28.3 (C-2), 26.2 (C-12), 21.3 (C-11), 19.5 (C-30), 18.8 (C-6), 16.5 (C-26), 16.4 (C-25), 16.3 (C-24), 15.0 (C-27) (Eder et al., 2008; Esposito et al., 2013).

2.3.1.6. Taraxerol (*6*)

Further elution using hexane-CH_2Cl_2 (70:30, v/v) gave a white crystal of (**6**), yield 7.6 mg; m.p. 282-284 °C; ^{13}C-NMR (CD_2Cl_2; 125MHz): δ 154.4 (C-20), 107.1 (C-30), 78.9 (C-3), 55.3 (C-5), 50.4 (C-9), 48.5 (C-18), 41.9 (C-14), 40.8 (C-8), 39.2 (C-22), 39.1 (C-16), 38.9 (C-1), 38.8 (C-4), 38.7 (C-13), 38.2 (C-19), 37.0 (C-10), 34.4 (C-17), 34.0 (C-7), 27.9 (C-23), 27.3 (C-2), 26.6 (C-15), 26.3 (C-28), 25.5 (C-12), 25.4 (C-21), 21.3 (C-11), 19.6 (C-29), 18.2 (C-6), 16.1 (C-26), 15.8 (C-25), 15.2 (C-24), 14.7 (C-27), (Yen et al., 2013).

2.4. *In vitro* anti-inflammatory activity by protein denaturation assay

The reaction mixture consisted of 2.8 mL of phosphate buffer saline (pH 6.4), 0.2 mL of bovine serum albumin (1 mg/mL) and 2 mL of different concentration (50, 100, 200, 400, 800 µg/mL) of methanol crude extract, compound (**1**), and aspirin as standard was incubated at 37 ± 2 ºC for 15 min. Denaturation was induced by keeping the reaction mixture at 70 ºC in a water bath for 10 min. After cooling, turbidity was measured spectrophotometrically at 660 nm (Shimadzu, UV1800). For negative control, 2 mL bovine serum albumin and 2.8 mL phosphate buffer saline (pH 6.3) were used. Each experiment was done in triplicate and the average was taken. The percentage inhibition of protein denaturation was calculated by using the following formula (Eqn.1) (Saso et al., 2001).

% Inhibition = [(absorbance of test sam.p.le − absorbance of control)/absorbance of control] × 100 (Eqn.1)

The compound/standard drug concentration for 50% inhibition (IC_{50}) was determined by plotting percentage inhibition with respect to control against treatment concentration.

2.5. Statistical analysis

The results were expressed as mean ± SD and statistical analysis was carried out by analysis of variance (ANOVA) followed by Duncan's multiple tests in which $p < 0.05$ was a criterion to be considered indicating significance as compared to the control group. All calculations were performed using SPSS package version17.0 (SPSS Inc., Chicago, Illinois, USA).

3. Results and Discussion

3.1. Spectroscopic characteristics of compound (**1**)

Compound (**1**) named 2-(7'-methylhexyloxy)furan-5'-yl)-6-(pyrrolidin-7-yl)piperazine responded positively using Dragendorff's reagent. The high resolution mass spectroscopy HR-ESIMS (positive mode) showed pseudo molecular ions peaks at *m/z* = 336.2575 $[M+H]^+$ and *m/z* = 358.2395 $[M+Na]^+$ (calcd. 358.2470) compatible with $C_{19}H_{33}N_3O_2$, accounting for five degrees of unsaturation (see Fig. S1). Its IR spectrum indicated distinctive absorption bands for secondary amine (υmax = 3341 cm^{-1}), olefin (υmax = 1550 cm^{-1}) and long aliphatic chain (υmax = 720 cm^{-1}) functionalities. The broad band decoupled ^{13}C NMR and DEPT 135 spectra displayed 19 carbon signals. These spectra indicated the presence of two primary sp^3 methyl carbons; nine methylene sp^3 carbons among which three bounded to a nitrogen and one to an oxygen atom; six methines with four sp^3 carbons among which three bounded to a nitrogen atom and two sp^2 carbons (Fig. S3).

The ^{1}H NMR spectrum of (**1**) revealed the presence of two methines protons at δ 4.51 (1H, dt, *J* = 6.2, 3.1 Hz, H-2), δ 4.35 (1H, dt, *J* = 6.5, 3.3 Hz, H-6) and two methylene diastereotopic protons at δ 2.22 (1H, m, H-3a), 2.05 (1H, m, H-3b), 2.47 (1H, m, H-5a), 2.14 (1H, m, H-5b) (Table 1) bounded to a nitrogen atom. This

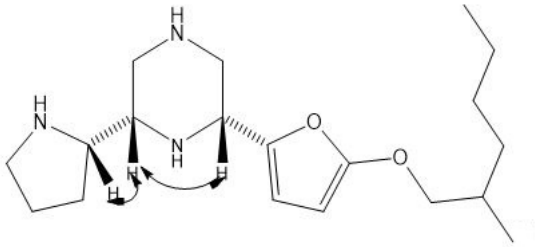

Fig. 4. Selected NOESY Correlations of 2-(7'-methylhexyloxy)-furan-5'-yl-6-(pyrrolidin-7-yl)piperazine (**1**).

Table 1

^{1}H NMR (500 MHz, ($CDCl_3$), ^{13}C NMR (125 MHz, ($CDCl_3$) data, coupling constant *J* in Hz in parentheses, and ^{1}H-^{13}C long-range HMBC correlation for 2-(7'-methylhexyloxy)-furan-5'-yl-6-(pyrrolidin-7-yl)piperazine (**1**).

	Attribution	Chemical shift δ in ppm		HMBC
		δH (*J* = Hz)	δC	
1				C-6, C-4′
2		4.51 , dt, (*J* = 6.2, 3.1)	56.8	C-5′, C-5
3	H-3a	2.22, m	46.3	C-3, C-7
	H-3b	2.05, m		C-2, C-11
5	H-5a	2.47, m	47.1	C-5 , C-9
	H-5b	2.14, m		
6		4.35, dt, (*J* = 6.5, 3.3)	55.8	
7		4.64, dt, (*J* = 7.5, 6.3)	57.8	
8				
9		2.37, m	45.5	
10		1.18, m	30.9	
11		1.28, m	30.2	
1′				
2′			168.1	
3′		7.58, d, (*J* = 5.3)	128.8	
4′		7.73, dd, (*J* = 5.3, 3.3)	130.9	
5′			133.2	
6′		4.22, dd, (*J* = 11.4, 5.7)	68.5	
7′		1.70, m	39.3	
8′		1.33, m	24.3	
9′		1.24 , m	23.5	
10′		1.27, m	29.4	
Me-11′		0.95, t, (*J* = 7.1)	11.3	
Me-12′		0.93, d, (*J* = 7.9)	14.3	

hypothesis was confirmed by the ^{13}C NMR of (**1**) which showed two methines carbons at δ 56.8 (C-2), δ 55.8 (C-6) and two methylenes carbons at δ 46.3 (C-3), δ 47.1 (C-5) bounded to a nitrogen atom. All these data strongly suggest the presence of a piperazine ring (see Fig.s S4, S5, S6) (Mamat et al., 2016; Wodtke et al., 2018). The hydrogen-hydrogen coupling constant observed for protons H-2 and H-6 was similar to piperidine alkaloids derivatives (Marcos et al., 2014) suggesting that the two fragments linked to piperazine link adopted equatorial position because of the chair constellation.

Besides, the presence of pyrrolidine ring was verified according to the ^{1}H NMR and ^{13}C NMR spectrum. It showed a methine proton at δ 4.64 (1H, dt, *J* = 7.5, 6.3 Hz, H-7) and methylene protons at δ 2.37 (2H, m, H-9) bounded to a nitrogen atom together with two other methylene protons at δ 1.18 (2H, m, H-10), δ 1.28 (2H, m, H-11). This was corroborated in ^{13}C NMR spectrum which indicated methines signals at δ 57.8 (C-7), δ 45.5 (C-5) bounded to a nitrogen atom and two others methylene signals at δ 30.9 (C-10), 24.3 (C-11) (see Fig.s S4, S5, S6). Pattern connectivities observed from COSY spectrum between H-2/H-3, H-6/H-7, H-6/H-5, H-7/H-11 (Fig. S8) and HMBC spectrum correlations between H-7 (δ 4.64) and C-5 (δ 46.3); H-7 (δ 4.64) and C-9 (δ 45.5); H-6 (δ 4.35) and C-11 (δ 30.2) were indicative the attachment of a pyrrolidine ring at C-6 to piperazine ring (Fig. S7) (Mikhova et al., 1987; Perumal et al., 2014).

In addition, the ^{1}H NMR spectrum showed the aromatic protons at δ 7.58 (1H, d, *J* = 5.3 Hz, H-3'), δ 7.73 (1H, dd, *J* = 5.3, 3.3 Hz, H-4') (Song et al., 2008; Liu et al., 2010; Yun et al., 2014) with their corresponding carbons signals at δ 128.8 (C-3'), 130.9 (C-4'), δ 168.1 (C-2') assigned to a quaternary sp^2 carbon bearing an oxygen atom and the COSY spectrum coupling between H-3'/H-4' revealed a furan skeleton (Song et al., 2008; Liu et al., 2010; Yun et al., 2014) (Fig.s S3, S4, S8). According to these data, compound (**1**) consisted of furyl-pyrrolidinyl-piperazine moiety in the coupling pattern and most of the chemical shifts. This was confirmed by EI mass spectrum which shows a peak at *m/z*=150 corresponding to furyl-piperazine fragment (Fig. S2). The attachment of furan ring was determined to be at C-2 of (**1**) in the HMBC spectrum which showed correlations from C-2 (δ 56.8)/H-3' (δ 7.58), C-5' (δ 133.2)/H-3b (δ 2.05) (Fig. S7). Besides, the ^{1}H NMR exhibited signals of a side chain of oxymethylene at δ 4.22 (2H, dd, *J* = 5.7, 11.4 Hz, H-6'), a methine group at δ 1.70 (1H, m, H-7'), three methylene groups at δ 1.33 (2H, m, H-8'), 1.24 (2H, m, H-9'), 1.27 (2H, m, H-10') along with two methyl groups at δ 0.95 (3H, t, *J* = 7.1 Hz, Me-11') and 0.93 (3H, d, *J* = 7.9 Hz, Me-12') (Song et al., 2008; Liu et al., 2010; Yun et al., 2014; Tamekoa et al., 2017). This was confirmed by the broad band decoupled ^{13}C NMR spectrum which revealed an oxymethylene carbon at δ 68.5 (C-6', CH_2O), a methine group at δ 39.3 (C-7'), three methylene groups at δ 24.3 (C-8'), 23.5 (C-9'), 29.4 (C-10') and two methyl groups at δ 11.3 (C-11') and 14.3 (C-12') (Song et al., 2008; Liu et al., 2010; Yun et al., 2014; Tamekoa et al., 2017). The presence of the butyl side chain was substantiated by the appearance of the base peak in the EI mass spectrum at *m/z* 279 $(M-C_4H_8)^+$ (Fig. S2). This methylhexyloxy fragment was linked to C-2' of the furan ring according to the HMBC correlations from C-2' (δ 168.1)/H-6' (δ 4.22) (Fig. S7). The COSY pattern connectivities observed indicated close spatial proximity of all protons (Fig. S8). The relative stereostructure at C-2, C-6, and C-7 of (**1**) was assigned mainly on the basis of hydrogen-hydrogen coupling constants data and NOESY experiment; The strong NOESY correlation observed between H-2 (δ 4.51)/ H-6 (δ 4.35) and H-6 (δ 4.35)/ H-7 (δ 4.64) (Fig. 4, Fig. S9, S10) suggested their β-orientation (Mitsuo et al., 1998; Viegas et al., 2004; Marcos et al., 2014). On the basis of these evidences, the structure of (**1**) was established as 2-(7'-methylhexyloxy)-furan-5'-yl-6-(pyrrolidin-7-yl)piperazine (Fig. 2).

The strong NOESY correlation observed between H-2 (δ 4.51)/ H-6 (δ 4.35) and H-6 (δ 4.35)/ H-7 (δ 4.64) (Fig. 4, Fig. S9 and Fig. S10) suggested their β-orientation (Mitsuo et al., 1998; Viegas et al., 2004; Marcos et al., 2014). On the basis of these evidences, the structure of (**1**) was established as 2-(7'-methylhexyloxy)-furan-5'-yl-6-(pyrrolidin-7-yl)piperazine (Fig. 2).

3.2. *In vitro* anti-inflammatory activity determination by protein denaturation assay

In the present investigation, the *in vitro* anti-inflammatory effects of the methanol extract and compound (**1**) were evaluated against denaturation of serum albumin. The results are shown in (Fig. 5). Compound (**1**) showed a significant activity with an IC_{50} of 1.930 ± 0.9123 µg/mL, while the extract revealed a slightly higher percentage of inhibition with an IC_{50} of 2.461 ± 0.9923 µg/mL compared to aspirin used as standard with an IC_{50} of 2.536 ± 0.9366 µg/mL. These results are in agreement with previously reported of similar vasodilator activity of piperazine derivatives (Regnier et al., 1968).

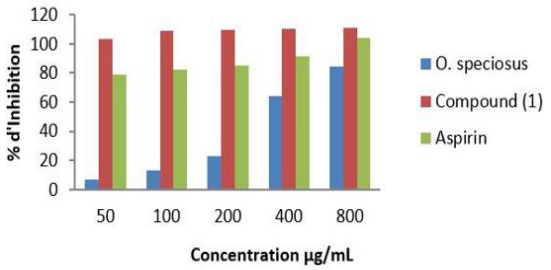

Fig. 5. *In vitro* anti-inflammatory activity of the methanol extract and compound (**1**). Values are mean of three replicate determinations (n = 5) mean ± standard deviation.

This probably explains the use of extracts from this plant by traditional healers against a certain number of inflammatory diseases because anti-inflammatory

activity seems to be related to the presence of pyrrolidinyl-piperazine skeleton since alkaloids are known to have anti-inflammatory property (Sotnikova et al., 1997).

4. Concluding remarks

The present study afforded the isolation and identification of a new natural product, namely 2-(7′-methylhexyloxy)-furan-5′-yl-6-(pyrrolidin-7-yl)piperazine (**1**), along with five known compounds involving aridanin (**2**), taraxeryl acetate (**3**), hexadecanoic acid (**4**), taraxerol (**5**), betulinic acid (**6**) from the roots of *O. speciosus* and therefore enhanced understanding about the phytoconstituents of this plant. The alkaloid derivative showed potent anti-inflammatory activity by protein denaturation assay compared to aspirin as standard and holds promise in the development of the lead-compound based anti-inflammatory therapeutics in the future.

Conflict of interest

The authors declare that there is no conflict of interest.

Acknowledgements

The authors are thankful to the instrumentation analytical facility of the Department of Organic Chemistry-NMR service of the University of Geneva for recording spectral data of the isolated compounds.

References

Adjanohoun, E.J., Ahyi, A.M.R., Ake, A.L., Baniakina, J., Chinon, P., Cusset, G., Doulou, V., Enzanza, A., Eymé, J., Goudoté, E., Keita, A., Mbemba, C., Mollet, J., Moutsaboté, J., M.p.ati, J., Sita, P., 1988. Contribution aux Etudes Ethnobotaniques et Floristiques en République Populaire du Congo. A.CC.T., Paris 605-606.

Aké, A.L., Abeye, J., Guinko, S., Riguet, R., Bangavou, X., 1985. Médecine traditionnelle et pharmacopée-Contribution aux études ethnobotaniques et floristiques en République Centrafricaine. A.C.C.T. Paris, France. pp. 140.

Aro, A.O., Dzoyem, J.P., Hlokwe, T.M., Madoroba, E., Eloff, J.N., Mcgaw, L.J., 2015. Some south African rubiaceae tree leaf extracts have antimycobacterial activity against pathogenic and non-pathogenic *Mycobacterium* species. Phytother. Res. 10, 1004-1010.

Aro, A.O., Dzoyem, J.P., Goddard, A., Fonteh, P., Kayoka-Kabongo, P.N., McGaw, L.J., 2019b. *In vitro* Antimycobacterial, apoptosis-inducing potential, and immunomodulatory activity of some Rubiaceae species. Front. Pharmacol. 10(185), 1-13.

Aro, A.O., Dzoyem, J.P., Awouafack, M.D., Selepe, M.A., Eloff, J.N., McGaw, L.J.A., 2019a. Fractions and isolated compounds from *Oxyanthus speciosus* subsp. *stenocarpus* (Rubiaceae) have promising antimycobacterial and intracellular activity. BMC Complement. Altern. Med. 19(108), 1-11.

Burkill, H.M., 1997. The Useful Plants of West Tropical Africa. 2nd Edition. Vol. 4, Families M-R. Royal Botanic Gardens, Kew, Richmond, United Kingdom.

Bouquet, A., 1969. Féticheurs et Médecine Traditionnelle du Congo (Brazzaville). Travaux et Documents de l'ORSTOM, Paris 36, 128.

Eder, B., Walmir, S.G., Lidilhone, H., Tieppo, C., Fernanda, R.G., 2008. Bioactive pentacyclic triterpenes from the stems of *Combretum laxum*. Molecules 13, 2717-2728.

Esposito, F., Sanna, C., Vecchio, C.D., Cannas, V., Venditti, A., Corona, A., Bianco, A., Serrilli, A.M., Guarcini, L., Parolin, C., Ballero, M., Tramontano, E., 2013. *Hypericum hircinum* L. components as new single-molecule inhibitors of both HIV-1 reverse transcriptase-associated DNA polymerase and ribonuclease H activities. Pathog. Dis. 68(3), 116-124.

Kokwaro, J.O., 1993. Medicinal Plants of East Africa. 2nd Ed. Kenya Literature Bureau, Nairobi, Kenya. 401 pp.

Liu, J., Xu, J., Zhao, J.X., Gao, Y.W., Zhang, Z.S., Guo, Q.Y., 2010. A new heterocyclic compound from *Cyathula officinalis* Kuan. Chin. Chem. Lett. 21, 70-72.

Mamat, C., Pretze, M., Gott, M., Köckerling, M., 2016. Synthesis, dynamic NMR characterization and XRD studies of novel *N,N´*-substituted piperazines for bioorthogonal labeling. Beilstein J. Org. Chem. 12, 2478-2489.

Marcos, P., Luciene, R.B., Abhinay, S., Myna, N., Amanda, D., Claudio, V.J., Celia, R.S.G., Vanderlan, S.B., 2014. Antimalarial activity of piperidine alkaloids from *Senna spectabilis* and semisynthetic derivatives. J. Braz. Chem. Soc. 25(10), 1900-1906.

Mikhova, B., Spassov, S.L., Popandova, K., Dryanska, V., Ivanov, C., Duddeck, H., Kaiser, M., 1987. NMR spectra and stereochemistry of some 2,3,4,5-tetrasubstituted pyrrolidines. J. Mol. Struct. 161, 1987, 231-235.

Mitsuo, M., Kimio, Y., Yukio, I., Hiromu, K., 1998. Insecticidal alkaloids against *Drosophila melanogaster* from *Nuphar japonicum* DC. J. Agric. Food. Chem. 46, 1059-1063.

Nahrstedt, A., Rockenbach, J., Wray, V., 1995. Phenylpropanoid glycosides, a furanone glucoside and Igeniposidic acid from members of the Rubiaceae. Phytochemistry 39(2), 375-378.

Neoh, B., Rahayu, U., Nordin, H., Tai, Y.C., Tu, Y.L., Mawardi R., Aspollah, S., 2010. Chemical constituents from two weed species of *Spermacoce* (Rubiaceae). Malaysian J. Anal. Sci. 14, 6-11.

Neuwinger, H.D., 2000. African Traditional Medicine: A Dictionary of Plant Use and Applications. Medpharm Scientific, Stuttgart, Germany, pp. 589.

Nzedong, T.I.B., Ngnokam, D., Tapondjou, A.L., Harakat, D., Voutquenne, L., 2010. Cycloartane glycosides from leaves of *Oxyanthus pallidus*. Phytochemistry 71, 2182-2186.

Nzedong, T.I.B., Ngnokam, D., Tapondjou, L.A., Harakat, D., Voutquenne, L., 2012. Isolation and caracterisation of sodium monocarboxylate ixoside salt from the stem bark of *Oxyanthus pallidus*. Int. J. Biol. Chem. Sci. 6(6), 7007-7012.

Olajide, O.O., Okwute, S.K., 2019. Stigmasterol and stigmasterol glycoside: Isolated compounds from *Tetrapleura tetraptera* extracts. J. Biochem. Int. 6(1), 21-48.

Rajakumar, P., Thirunarayanan, A., Raja, S., 2014. Syn-

thesis and antibacterial activity of novel *N*-methyl pyrrolidine dendrimers via [3+2] cycloaddition. Proc. Natl. Acad. Sci. India Sect. A Phys. Sci. 84, 371-379.

Raponda-Walker, A., Sillans, R., 1961. Les plantes utiles du Gabon. Paul Lechevalier, Paris, France. pp. 614.

Regnier, G.L., Canavari, R.J., Laubie, M.J., Le Douareg, J.C., 1968. Synthesis and vasodilator activity of new piperazine derivatives. J. Med. Chem. 11(6), 1151-1155.

Rockenbach, J., Nahrstedt, A., Wray, V., 1992. Cyanogenic glycosides from *Psydrax* and *Oxyanthus* species. Phytochemistry 31(2), 567-570.

Saso, L., Valentini, G., Casini, M., Grippa E., Gatto, M.T., Leone, M., Silvestrini, B., 2001. Inhibition of heat-induced denaturation of albumin by nonsteroidal antiinflammatory drugs (NSAIDs): Pharmacological im.p.lications. Arch. Pharm. Res. 24, 150-151.

Sotnikova R., Kettmann V., Kostalova D., Taborska E., 1997. Relaxant properties of some aporphine alkaloids from *Mahonia aquifolium*. Methods Find. Exp. Clin. Pharmacol. 19, 589-597.

Song, M.C., Yang, H.J., Jeong, T.S., Kim, K.T., Baek, N.I., 2008. Heterocyclic compounds from *Chrysanthemum coronarium* L. and their inhibitory activity on hACAT-1 hACAT- 2, and LDL-oxidation. Arch. Pharm. Res. 31, 573-578.

Tamekoa, M.J.E., Chouna, J.R., Nkeng-Efouet, A.P., Tapondjou, A.L., Sewald, N., 2017. Furan derivatives from *Lannea kerstingii*. Phytochem. Lett. 20, 282-284.

Trinh, T.T., Tran, V.S., Katrin, F., Ludger, W., 2008. Triterpenes from the roots of *codonopsis pilosula*. J. Chem. 46(4), 515-520.

Viegas Jr, C., Da S. Bolzani, V., Furlan, M., Barreiro, E.J., Young, M.C.M., Tomazela, D., Eberlin, M.N., 2004. Further bioactive piperidine alkaloids from the flowers and green fruits of *Cassia spectabilis*. J. Nat. Prod. 67, 908-910.

Wodtke, R., Steinberg, J., Kockerling, M., Loser, R., Mamat, C., 2018. NMR-based investigations of acyl-functionalized piperazines concerning their conformational behavior in solution. Roy. Soc. Chem. Adv. 8, 40921-40933.

Yen, C.K., Keng, C.W., Hasnah, O., Ibrahim, E., Mohammad, Z.A., 2013. Chemical constituents and biological activities of *Strobilanthes crispus* L. Rec. Nat. Prod. 7(1), 59-64.

Yun, H.M., Shu, X.J., Chen, G.Y., Ji, M.H., Ding, J.Y., 2014. Chemical constituents from barks of *Lannea coromandelica*. Chin. Herb. Med. 6, 65-69.